NEW OVERALL HEAT TRANSFER COEFFICIENT CORRELATION FOR EVAPORATIVE CONDENSERS

Ivoni C. Acunha Jr., ivoni.acunha@riogrande.ifrs.edu.br
Instituto Federal de Educação, Ciência e Tecnologia do Rio Grande do Sul – Rua Alfredo Huch, 475, Rio Grande - RS
Renato Pessini, rpessini@yahoo.com
Paulo Smith Schneider, pss@mecanica.ufrgs.br
Universidade Federal do Rio Grande do Sul, Rua Sarmento Leite, 425, Porto Alegre - RS

Abstract. *This work presents an experimental analysis for an evaporative condenser built in reduced scale, keeping the geometric similarity to a real size equipment. The reduced scale condenser has a bundle of 210 copper tubes, with 6mm of external diameter arranged in 35 columns and 6 tube passes, assembled inside a glass enclosure to allow for the water and air flows visualization. The condenser operates under different water and air mass flow rates and uses R-22 as the refrigerant fluid. The set of measured data is compared with similar ones available in the literature and allowing for analysis of heat transfer processes on the reduced scale evaporative condenser, one of the main goals of this work. Infrared thermography images enabled the identification of three heat transfer zones: desuperheating, condensation and subcooling. For the R-22 two phase flow, the local heat transfer coefficient is determined as a function of the vapor quality and compared to an average coefficient. The methodology of analysis consists on the determination of the flow pattern map, followed by the calculation of the transition regions based on the void fraction concept. The flow patterns are classified as fully stratified and the condensation model assumes that two types of heat transfer mechanisms occur within the tubes: film condensation and convective condensation. As a conclusion, a new overall heat transfer coefficient based on geometric and operational conditions of the evaporative condenser is proposed, taking into account the heat transfer contributions of the desuperheating and subcooling single phases . The proposed correlation presents a maximum deviation about 10% to experimental values.*

Keywords*: Heat transfer coefficient, evaporative condenser, convective condensation, film condensation*

1. INTRODUCTION

The analysis of equipments for fluid refrigerant condensation in large size refrigeration systems, especially those operating with R-717 and R-22 are of great importance and arouse interest, since condensers with better performances can reduce significantly initial and operational costs of the systems.

Detailed physical modeling offers great advantages when used for operation and performance analysis of equipments, and one of the main challenges is the establishment of more realistic heat transfer correlations. Following this goal, several works have been developed with the purpose of better understanding the heat and mass transfer phenomena of evaporative condensers and cooling towers.

A similar methodology was found in Facão (1999), who developed an experimental work on a 10 kW nominal capacity cooling tower with indirect contact, obtaining heat and mass transfer coefficients. The results were similar to those found by Parker and Treybal (1961) and Niitsu *et al*. (1967).

The main goal of this work is to propose new correlations for the heat transfer that takes place on evaporative condensers based on an experimental set of measurements obtained out of a reduced scale equipment, performed under environment controlled conditions. Local and average overall heat transfer coefficients are evaluated as a function of the condenser geometry and operational conditions. These new correlations can be helpful for the development of new evaporative condensers.

2. EXPERIMENTAL SETUP

An experimental rig was built around the reduced scale evaporative condenser in order to perform calorimetric essays at controlled environment conditions (Fig. 1). Heat is transferred to the refrigerant fluid (R-22) at the evaporator, flows across a liquid receiver before changing phase at the condenser, in a closed loop depicted at the same figure by a red line. R-22 was choose as the refrigerant fluid due to its lower toxicity in comparison to R-717, together with its low corrosion potential to copper materials.

Hot water (blue line loop at Fig. 1) is the heating source of the rig, generated by a 2.7 kW (nominal power) electric element. The green line represents the cooling water loop of the evaporative condenser.

The measuring positions of the most significant variables also are showed in this figure, and the symbols that represent them are: V (electrical tension, in volts), A (electrical current, in amperes), T_{DB} and T_{WB} (dry and wet bulb air temperatures, in ^{o}C), T (R-22 and water temperatures, in ^{o}C), P (pressure, in bar) and Q (volumetric flow rate, in m^3h^{-1}).The refrigerant flow rate is driven by the heat transfer rate in the evaporator. The control of the hot water temperature on the water tank is performed by a PID controller.

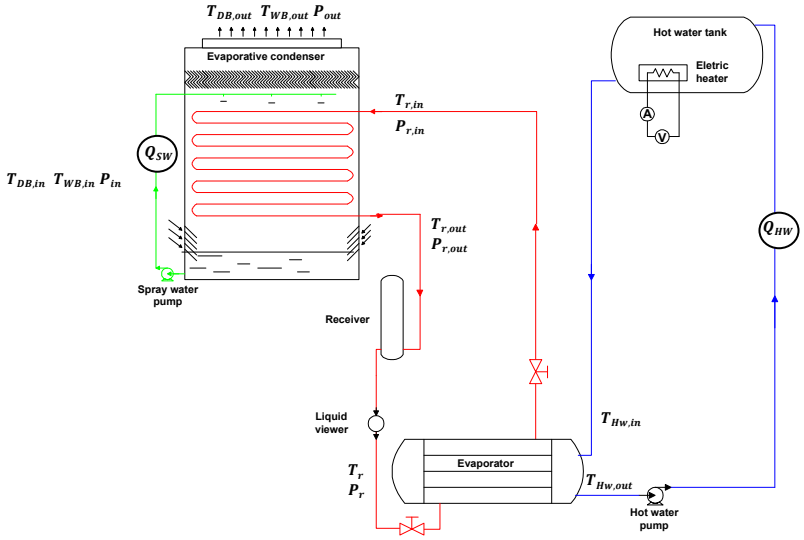

Figure 1. Test facility scheme

2.1. Evaporative condenser

The evaporative condenser was built keeping a geometric similarity to a commercially model, running on R-717 as refrigerant fluid in industrial refrigeration systems, with a scale factor of 1/4. The reduced scale evaporative condenser and its experimental setup are presented at Figs. 2a and 2b, respectively.

a) **b)**

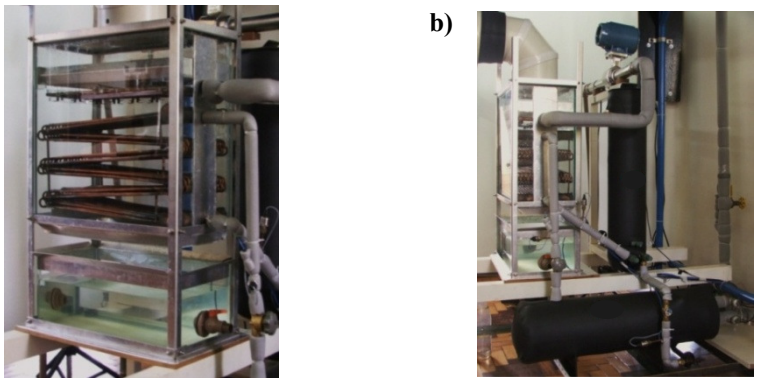

Figure 2. a) small scale evaporative condenser; b) experimental facility

Coil were built on copper tubes of 6.35mm external diameter (corresponding to commercial diameter of 1/4in), 35 columns of 6 tubes in a staggered arrangement, joined in a distributor at the top and in a collector at the bottom, with a total heat transfer area of 2.17 m^2.

A copper water spray distributor was placed above the coil, with 36 holes allowing for a uniform distribution of the spray on the outside surface of the coil. The spray water flow rate was controlled by a bypass placed on the pumping circuit. The drift eliminator was made in aluminum with spacing of 1.8 mm.

The air flow leaves the condenser through a 200 mm nominal diameter pipe connected to a centrifugal fan. The air flow rate was controlled by a frequency inverter acting on an electric driver. The water sump was made on glass and has a volume of 25 l. The water make up was added at the end of each measured sample, providing sump water with more homogeneous temperatures and helped keeping operation at steady state conditions.

2.2 Measurements

All measured points are depicted on Fig.1, and are described according to their fluid circuit relations. Starting with the air flow circuit, the ambient air dry and wet bulb temperatures ($T_{DB,in}$ and $T_{WB,in}$) are measured by two PT-100 sensors. The inlet and outlet air pressures (P_{in} and P_{out}), as well as dry and wet outlet bulb temperatures ($T_{DB,out}$ and $T_{WB,out}$) are measured with a Vaisala PTU – 303 meter. The volumetric air flow rate is measured by a Venturi tube.

For the R-22 circuit, the inlet and outlet temperatures ($T_{r,in}$ and $T_{r,out}$) and pressures ($P_{r,in}$ and $P_{r,out}$) are measured for the superheated vapor and subcooling liquid phases, respectively. Also, pressure and temperature of the refrigerant fluid are measured between the liquid receiver and the evaporator Although this temperature is taken at the pipe external surface , its measurement is worth to check its approximate expected value and the adiabatic behavior of the system. These temperatures are measured by type *J* thermocouples and the pressures with digital pressure transducers.

Spray water circuit includes the measurement of the water spray temperature T_w, taken inside the water sump and simultaneously right before the sprinkling nozzles. Results showed then to be similar. Water spray flow rate (Q_{sw}) is measured by a volumetric flow meter.

Hot water circuit includes the measurement of the inlet and outlet hot water temperatures ($T_{Hw,in}$ and $T_{Hw,out}$) in the evaporator by type *J* thermocouples, and its volumetric flow rate (Q_{Hw}).

Finally, the refrigerant fluid mass flow rate ($\dot{m}_r$) is determined by the aid of a mass and energy balance around a control volume placed on the evaporator. The heat transfer involved in the process can also be determined by the electric power delivered to the hot water electric heater and by the air side, to compare results and ensure the measurement reliability.

Further details about sensors calibration and measuring uncertainty can be seen in Acunha *et al*. (2010).

3 Heat transfer rate

To evaluate the thermal capacity of an evaporative condenser, ambient heat transfer rate, or rejected heat $\dot{q}$ (kW), must be determined. This heat transfer rate can be calculated by two ways. The first one is performed by the thermal balance involving the water spray and the air flow streams, as represented in Eq (1) (ASHRAE, 2005).

$$\dot{q} = \dot{m}_{air}\left(h_{air,out} - h_{air,in}\right) - \dot{m}_{wmu}h_w \tag{1}$$

where $\dot{m}_{air}$ is the air mass flow rate across the evaporative condenser (kg s^{-1}), $h_{air,in}$ and $h_{air,out}$ are, respectively, the air specific enthalpies in the inlet and outlet of evaporative condenser (kJ kg^{-1}), $\dot{m}_{wmu}$ is the make up water mass flow rate (kg s^{-1}) and h_w is the sump water enthalpy (kJ kg^{-1}).

The second one is based on the a thermal balance among the refrigerant and make up water flows (ANSI/ASHRAE, 1995) which has the same heat transfer rate in the evaporator

$$\dot{q} = \dot{m}_r\left(h_{r,in} - h_{r,out}\right) - \dot{m}_{wmu}(h_w - h_{wmu}) = \dot{m}_{Hw}\left(h_{Hwr,in} - h_{Hwr,out}\right) \tag{2}$$

where $\dot{m}_r$ and $\dot{m}_{Hw}$ are, respectively, the refrigerant and hot water mass flow rates (kg s^{-1}), $h_{r,in}$ and $h_{r,out}$ are, respectively, the refrigerant specific enthalpies (kJ kg^{-1}) in the inlet and outlet of tube bundle and h_{wmu} is the make up water specific enthalpy (kJ kg^{-1}). The hot water specific enthalpies ($h_{Hwr,in}$ and $h_{Hwr,out}$) are determined from measured pressures and temperatures at the evaporator. Eq. (2) enables to calculate the heat transfer rate and the refrigerant mass flow rate.

After the heat transfer is determined, the experimental overall heat transfer coefficient, U_{exp} (Wm^{-2} °C^{-1}) can be calculated, through equations 3 and 4

$$U_{exp} = \frac{\dot{q}}{A\,\Delta T_{exp}} \tag{3}$$

$$\Delta T_{exp} = T_{cond} - T_w \tag{4}$$

where A is the outside surface area of tubes (m^2) and, T_{cond} and T_w are the refrigerant fluid condensation and spray water temperatures (°C), respectively.

In this work, the overall heat transfer coefficient is calculated for three heat transfer zones: desuperheating, condensation and subcooling, which are determined through infrared (IR) thermografic images. Figure 3 shows an IR thermografic image where these three zones can be seen. The lower limit in the scale temperature in this picture corresponds to the R-22 condensation temperature. Therefore, the R-22 subcooling zone do not appears and can be seen a black image for this region.

The R-22 desuperheating region appears just in the condenser distributor while the R-22 subcooling occurs in approximately 2/5 of the last tubes pass. The remaining area is where the refrigerant fluid condensation takes place.

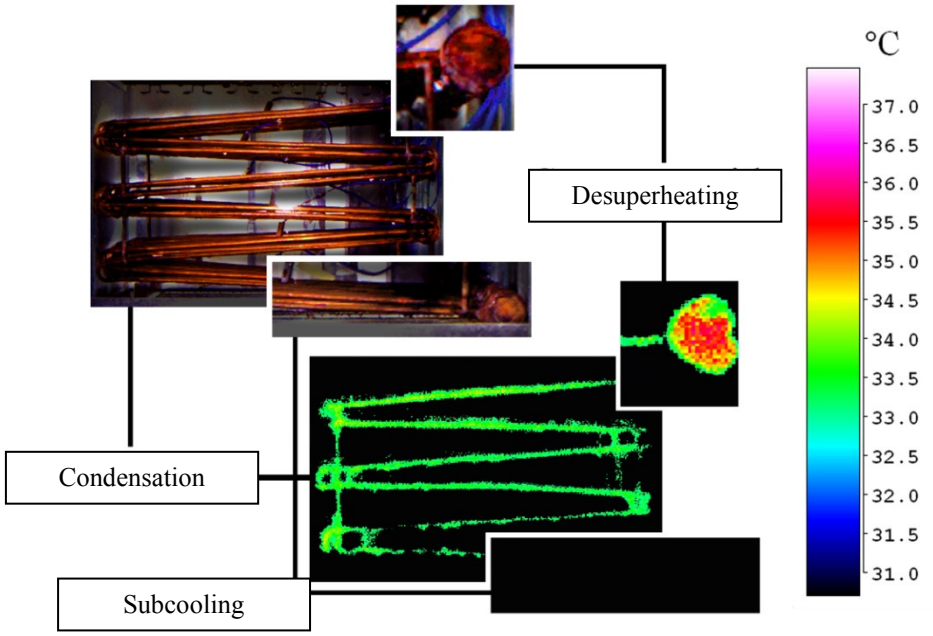

Figure 3. Three heat transfer zones of the evaporative condenser identified by infra red thermography

For all zones, the heat transfer rate is determinate both experimentally (Eq. (1)) and theoretically by correlations. The stronger influence is verified for the condensate zone, which covers the largest heat transfer area. Figure 4 shows the product of experimental overall heat transfer coefficient (U_{exp}) by heat transfer area (A) for 40 measuring samples. The values of $U_{exp}A$ for the condensation zone are significantly higher than those for the other two regions, and therefore the greater attention will be focused on this region.

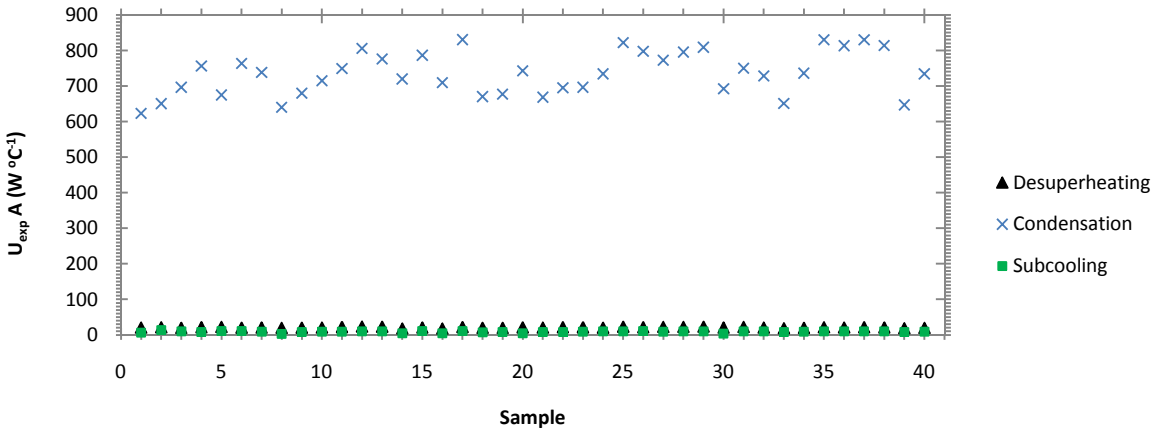

Figure 4. Product of the overall heat transfer by area for the three heat transfer sones of the evaporative condenser

Figure 5 depicts a scheme of the refrigerant, spray water and air flows over an elementary cross section of a tube. For simplicity, the refrigerant and spray streams flows are at the same sense.

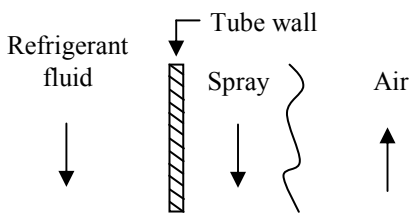

Figure 5. Schematic water, refrigerant and air flows over a tube

The overall heat transfer coefficient is calculated for that region by Equation (5), in respect to the outer diameter d_{ext} (ASHRAE, 2000)

$$U = \frac{1}{\frac{d_{ext}}{d_{\text{int}}}\left(\frac{1}{h_{\text{int}}}\right)+\frac{d_{ext}}{d_m}\left(\frac{L}{k_T}\right)+\frac{1}{h_{ext}}} \tag{5}$$

where k_T is the tube thermal conductivity (W m^{-1} °C^{-1}), d_{int} and d_{ext} are the internal and external tube diameter (m), respectively, d_m is the mean tube diameter (m), L is the tube thickness (m), h_{int} is the heat transfer coefficient between the refrigerant fluid and the internal tube surface (W m^{-2} °C^{-1}) and h_{ext} is the heat transfer coefficient between the external tube surface and the water spray (W m^{-2} °C^{-1}).

3.1 Refrigerant fluid heat transfer coefficient

The internal heat transfer coefficient h_{int} can be evaluated as an average or a local value. The local value must be a function of the refrigerant fluid properties, evaluated at its single phase temperatures. The Dittus- Boelter (1985, reprinted version, *appud* Bejan, 1995) correlation is used to estimate h_{int} for the desuperheating and subcooling regions:

$$Nu = \frac{h_{int}d_{int}}{k} = 0.023Re^{4/5}Pr^{n} \tag{6}$$

where k is the refrigerant thermal conductivity (W m^{-1} °C^{-1}), *Nu, Re* and *Pr* are the Nusselt, Reynolds and Prandtl numbers. The exponent of the Prandtl number (n) is 0.3 for desuperheating and subcooling zones.

For the average heat transfer coefficient, the thermophysical properties in Eq. (6) are evaluated at the refrigerant fluid mean temperature, taken at the inlet and outlet considered regions.

The flow map pattern, which is a function of the void fraction, is mandatory information in order to estimate the local heat transfer coefficient in the two phase zone, as it changes with vapor quality.

El Hajal *et al*. (2003) proposed a new version of a two phase flow pattern map for condensation inside horizontal plain tubes, based on the original work of Kattan *et al*. (1998) for boiling flow model, completed by Thome *et al*.(2003) to determinate the local heat transfer coefficient.

More recently, flow patterns are classified as: fully stratified flow, stratified wavy flow, intermittent flow, annular flow, mist flow and bubbly flow. However, considering that condensation in this work is a gravity controlled process, the flow occurs at very low mass velocities and a fully stratified flow in all measured samples were verified. In this case, when the saturated vapor enters a condensation zone, it forms a liquid layer at the bottom of the tube and a condensing film around the upper tube perimeter. Thus, the heat transfer coefficient must account for these two transport mechanisms.

Figure 6a shows a flow map pattern while Fig 6b shows the convective condensation (related to h_c) and film condensation (related to h_f) and their respective heat transfer surface area. All measuring samples of this study presented mass velocities below the limit transition between fully stratified flow and stratified wavy flow. Therefore, all analysis and equations were performed for fully stratified flows.

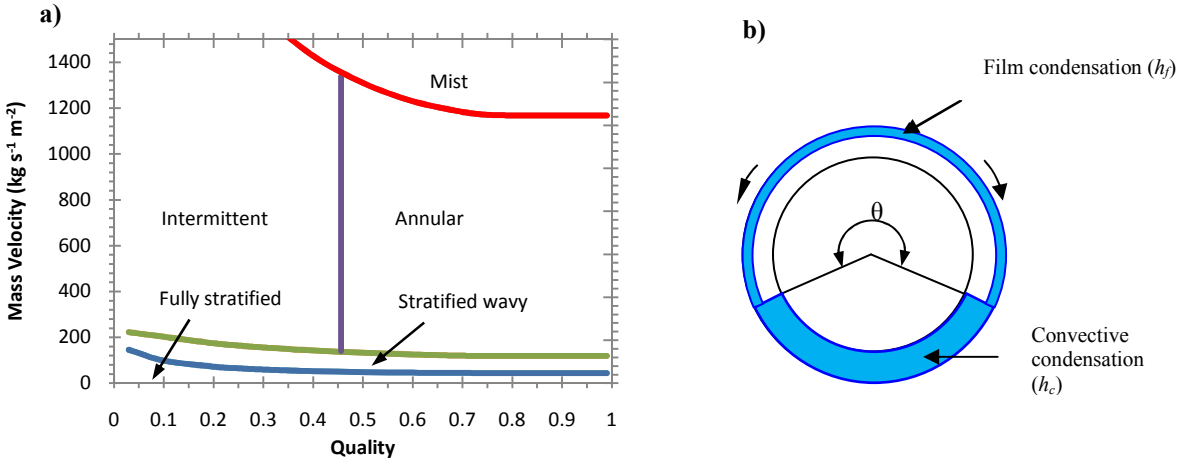

Figure 6. a) Condensation map for R-22 flowing inside a tube; b) Heat transfer coefficients and their respective perimeters (Adapted from Thome e*t al*. (2003)).

The θ angle (rad) in this case is the stratified angle and defines the regions where the heat transfer coefficients must be related to the film condensation type or of the convective condensation type. Thus, for a tube radius r, the internal heat transfer coefficient h_{int} (W m^{-2} ^{o}C^{-1}) is:

$$h_{int} = \frac{r\theta h_f + (2\pi - \theta) r h_c}{2\pi r} \tag{7}$$

A non iterative equation can be used to determine the θ angle, as a function of the void fraction, ε

$$\theta = 2\pi - 2\left[\pi(1-\varepsilon) + \left(3\frac{\pi}{2}\right)^{1/3}\left[1 - 2(1-\varepsilon) + (1-\varepsilon)^{1/3} - \varepsilon^{1/3}\right] - \frac{1}{200}(1-\varepsilon)\varepsilon\left[1 + 4\left((1-\varepsilon^2) + \varepsilon^2\right)\right]\right] \tag{8}$$

The void fraction ε is a logarithmic mean between homogeneous void fraction (ε_h) and the non homogeneous drift flux void fraction model of Rouhani and Axelsson (1970) (ε_{ra}). These void fraction calculations are performed by the following equations:

$$\varepsilon_h = \left[1 + \left(\frac{1-x}{x}\right)\frac{\rho_L}{\rho_v}\right]^{-1} \tag{9}$$

$$\varepsilon_{ra} = \frac{x}{\rho_v}\left([1 + 0.12(1-x)]\left[\frac{x}{\rho_v} + \frac{1-x}{\rho_L}\right] + \frac{1.18(1-x)\left[g\sigma(\rho_L - \rho_v)^{0.25}\right]}{G{\rho_L}^{0.5}}\right)^{-1} \tag{10}$$

$$\varepsilon = \frac{\varepsilon_h - \varepsilon_{ra}}{ln\left(\frac{\varepsilon_h}{\varepsilon_{ra}}\right)} \tag{11}$$

where ρ_l and ρ_v are, respectively, the liquid and vapor densities (kg m^{-3}), x is the vapor quality, g is the acceleration of gravity (m s^{-2}), σ is the surface tension (N m^{-1}) and G is the mass velocity (kg s^{-1} m^{-2}).

Knowing the tube internal cross sectional area A (m^2) and the void fraction, the tube cross sectional area occupied by both liquid and vapor (A_L and A_v, in m^2) and liquid thickness (δ, in m) can be determined from

$$A_L = A(1-\varepsilon) \tag{12}$$

$$A_L = A\varepsilon \tag{13}$$

$$\mathrm{A_L} = \frac{1}{8}(2\pi - \theta)[\mathrm{d_{int}} - (\mathrm{d_{int}} - 2\delta)^2] \tag{14}$$

Convection heat transfer coefficient h_c (W m^{-2} ^{o}C^{-1}) is defined as:

$$h_c = 0.003 Re_L^{0.74} Pr_L^{0.5} \frac{k_L}{\delta} f_i \tag{15}$$

The Reynolds and Prandtl numbers for the liquid phase (Re_L and Pr_L) and the interfacial roughness factor (fi), are calculates by

$$Re_L = \frac{4\mathrm{G(1-x)}\delta}{(1-\varepsilon)\mu_\mathrm{L}} \tag{16}$$

$$Pr_L = \frac{4G(1-x)\delta}{(1-\varepsilon)\mu_L} \tag{17}$$

$$f_i = 1 + \left(\frac{u_v}{u_L}\right)^{1/2}\left[\frac{(\rho_L - \rho_v)g\delta^2}{\sigma}\right]^{1/4}\left(\frac{G}{G_{strat}}\right) \tag{18}$$

where μ_L is the dynamic viscosity (N s m^{-2}), k_L is the thermal conductivity (W m^{-1} ^{o}C^{-1}), C_{pL} is the specific heat, G_{strat} is the stratified flow transition mass velocity (kg s^{-1} m^{-2}), all for the liquid phase. The mean velocities u_L and u_v (m s^{-1}) refers to the liquid and vapor phases, respectively. Equations (19), (20) and (21) are used in order to calculate G_{strat}, u_L and u_v

$$G_{strat} = \left[\frac{(226.3)^2 \left(\frac{A_L}{d_{int}^2}\right)\left(\frac{A_v}{d_{int}^2}\right)^2 \rho_v(\rho_L - \rho_v)\mu_{Lg}}{x^2(1-x)\pi^3} \right]^{1/3} + 20x \quad (19)$$

$$u_v = \frac{Gx}{\rho_v \varepsilon} \quad (20)$$

$$u_L = \frac{G(1-x)}{\rho_L(1-\varepsilon)} \quad (21)$$

The film condensation heat transfer coefficient h_f, (W m^{-2} ^{o}C^{-1}) expresses a mean value evaluated over the upper perimeter of the tube, calculated by the Eq. (21). Thermophysical properties are evaluated at the mean value between tube wall and refrigerant saturation temperatures T_p and T_{sat}, respectively.

$$h_f = 0.728 \left[\frac{\rho_L(\rho_L - \rho_v) g h_{fg} k_L^3}{\mu_L d_{int}(T_{sat} - T_p)} \right]^{1/4} \quad (22)$$

In this equation h_{fg} is the latent heat of vaporization of the R-22 (J kg^{-1} ^{o}C^{-1}).

The average heat transfer coefficient is given by (Chato, 1962)

$$\bar{h}_{int} = 0.555 \left[\frac{\rho_L(\rho_L - \rho_v) g h'_{fg} k_L^3}{\mu_L d_{int}(T_{sat} - T_p)} \right]^{1/4} \quad (23)$$

where h'_{fg} is the R22 latent heat of vaporization h_{fg} (J kg^{-1} ^{o}C^{-1}) with a correction term that takes into account the effect of its subcooling, , as

$$h'_{fg} = h_{fg} + \frac{3}{8} c_{p,L}(T_{sat} - T_p) \quad (24)$$

3.2 Spray water heat transfer coefficient

Values for the heat transfer coefficient between external tube surfaces and water spray were calculated after some well known correlations available in the literature and compared to those obtained from experimental data.

Tovaras *et al*. (1984) (appud Zalewski and Gryglaszwski, 1997) proposed a correlation for this heat transfer coefficient as a function of the water Prandtl number (Pr_w) and the water and air Reynolds number (Re_w and Re_{air}). This correlation for water flowing downstream across horizontal tubes has the following form:

in the range: $690 < Re_{air} < 3000$, $Nu_w = 3.3 \times 10^{-3} Re_w^{0.3} Re_{air}^{0.15} Pr_w^{0.61}$;

in the range: $3000 < Re_{air} < 6900$, $Nu_w = 1.1 \times 10^{-2} Re_w^{0.3} Pr_w^{0.62}$;

for $Re_{air} > 6900$, $Nu_w = 0.24\ Re_w^{0.3} Re_{air}^{-0.36} Pr_w^{0.66}$

where:

$$Re_w = \frac{4\Gamma}{\mu_w} \quad (25)$$

$$Re_{air} = \frac{u_0 d_{ext} \rho_{air}}{\mu_{air}} \quad (26)$$

On these equations μ_w and μ_{air} are the dynamic viscosities of water spray and air (kg s^{-1} m^{-1}), ρ_{air} is the air density (kg m^{-3}), u_0 is the air velocity for the smallest cross area section (m s^{-1}), Γ is the spray water mass flow rate per unit length of tube in kg s^{-1} m^{-1} (Parker and Treybal, 1961). The external heat transfer coefficient (h_{ext}) is given by:

$$Nu_w = \left(\frac{v_w^2}{g}\right)^{1/3} \frac{h_{ext}}{k_w} \quad (27)$$

In this equation k_w is the spray water conductivity (Wm^{-1} ^{o}C^{-1}) and it is available for the range $160 < Re_w < 1360$ and $4.3 < Pr_w < 11.3$.

Parker and Treybal (1961) investigated evaporative condensers at 5 different situations, obtaining a correlation for the temperatures range of 15 to70 ^{o}C and $1.4 < \Gamma/d_{ext} < 3.0$ kg s^{-1} m^{-2} which is given by

$$h_{ext} = 704(1.39 + 0.022T_w)\left(\frac{\Gamma}{d_{ext}}\right)^{1/3} \quad (28)$$

Mizushina *et al*. (1967), developed a wider spectrum correlation than the former equation, within the range of $0.2 < \Gamma/d_{ext} < 5.5$ kg s^{-1} m^{-2}

$$h_{ext} = 2102.9\left(\frac{\Gamma}{d_{ext}}\right)^{1/3} \tag{29}$$

The correlation proposed by Leidenfrost e Korenic (1982) was developed for an inline bundle tube with an external diameter of 15.9 mm and is quite similar to Eq. (29)

$$h_{ext} = 2064\left(\frac{\Gamma}{d_{ext}}\right)^{0.252} \tag{30}$$

Niitsu *et al*. (1967) studied evaporative coolers with bare and finned tubes finding for the last one higher heat transfer coefficients for $0.5 < \Gamma/d_{ext} < 3.2$ kg s^{-1} m^{-2}

$$h_{ext} = 990\left(\frac{\Gamma}{d_{ext}}\right)^{0.46} \tag{31}$$

Very similar correlation was proposed by Dreyer and Erens (1990):

$$h_{ext} = 2843\left(\frac{\Gamma}{d_{ext}}\right)^{0.384} \tag{32}$$

The spray water heat transfer coefficients (h_{ext}) calculated with data of forty experimental samples allowed estimating the overall heat transfer coefficients $\overline{U}$, displayed in Fig 7. Samples were obtained under similar heat transfer rates, changing air and spray water flow rates, environmental laboratory conditions.

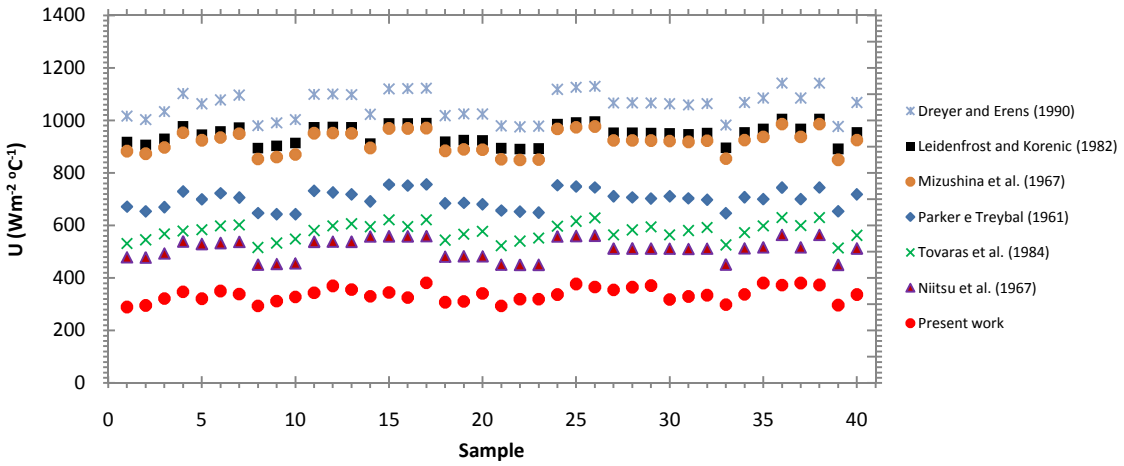

Figure 7. Overall heat transfer coefficients U for forty experimental samples using six external heat transfer coefficient from the literature and data from the present work

3 RESULTS AND DISCUSSION

Fig. 7 enables to observe the values of the overall heat transfer coefficient U obtained from six known correlations (equations 27 to 32) and a experimental one, based on data of the present work. The Niistu et al. (1967) correlation displayed the better agreement with the experimental data. Thus, this correlation was used to investigate the influence of the vapor quality on the overall and convection heat transfer coefficients.

Figure 8a shows a comparison between local and average internal convection heat transfer coefficients as well as local and average overall heat transfer coefficients for condensation zone. The local convection heat transfer coefficient present large difference in relation to the average coefficient mainly for vapor quality values close to 0 or 1. However, this trend is greatly relieved in the value of U_{cond}. In fact, it occurs because the scale of h_{ext} is lower of h_{int} scale and $\overline{U}_{cond}$ become of h_{ext} magnitude order.

The Niistu et al. (1967) correlation for h_{ext}, as well as other correlations, is a function of Γ/d_{ext}, basically. Thus, a new correlation based on this factor can be established for $\overline{U}_{cond}$ (Eq. (33)). Figure 8b shows the relationship between predicted $\overline{U}_{cond}$ and that theoretical obtained from Equations (5), (23) and (31) for the 40 measuring samples.

$$\overline{U}_{cond} = A + B\left(\frac{\Gamma}{d_{ext}}\right) - C\left(\frac{\Gamma}{d_{ext}}\right)^2 \tag{33}$$

where the A, B and C coefficients are, respectively, 279 W m^{-2} °C^{-1}, 647 J kg^{-1} °C^{-1} e 234 (J kg^{-1} °C^{-1}) (s m^2 kg^{-1}) and the subscript *cond* refers to condensation zone. In spite of the good agreement with theoretically calculated results, this correlation needs to be improved for better agreement to experimental data (Eq. (3)).

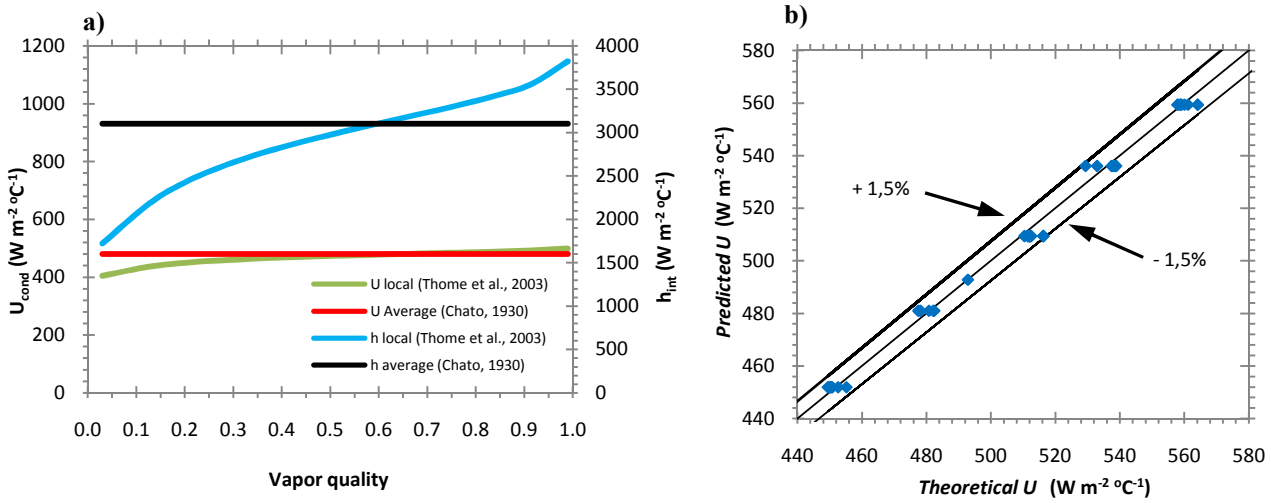

Figure 8. a) Convection and overall heat transfer coefficients; b) predicted and Theoretical $\overline{U}$

Actually, the evaporative condenser has two others zones (desuperheating and subcooling) that has influence on $\overline{U}$calculated just for condensation zone. The proposed correlation for $\overline{U}$ value must take account the heat transfer of these regions. Thus a correction factor (FC) can be introduced in order to get lower deviations. This correction factor is proportional to:

$$FC\ \alpha\ \frac{\overline{U}_{desup}}{\overline{U}_{cond}}\frac{\overline{U}_{sub}}{\overline{U}_{cond}}\overline{U}_{cond} \tag{34}$$

where the subscripts *desup* and *sub* refers to desuperheating and subcooling regions, respectively. Since that $\overline{U}$ is inversely proportional to differences of temperature between R-22 and spray water, $\overline{U}$ will be predicted by $U_{cond} - FC$

$$\overline{U} = \left[1 - \frac{(T_{cond} - Tw)}{(T_{r,in} - Tw)}\frac{(T_{cond} - Tw)}{(T_{r,out} - Tw)}\right]\overline{U}_{cond} \tag{35}$$

Another consideration is necessary because Γ is calculated to one tube row and the evaporative condenser has two passes per row. The final $\overline{U}$ correlation for whole condenser is

$$\overline{U} = \left[1 - \frac{(T_{cond} - Tw)}{(T_{r,in} - Tw)}\frac{(T_{cond} - Tw)}{(T_{r,out} - Tw)}\right]\left[279 + 323{,}5\left(\frac{\Gamma}{d_{ext}}\right) - 58{,}5\left(\frac{\Gamma}{d_{ext}}\right)^2\right] \tag{36}$$

Figure 9a shows a comparison between $\overline{U}$ predicted by proposed correlation and that obtained from measurements for the 40 measuring samples.

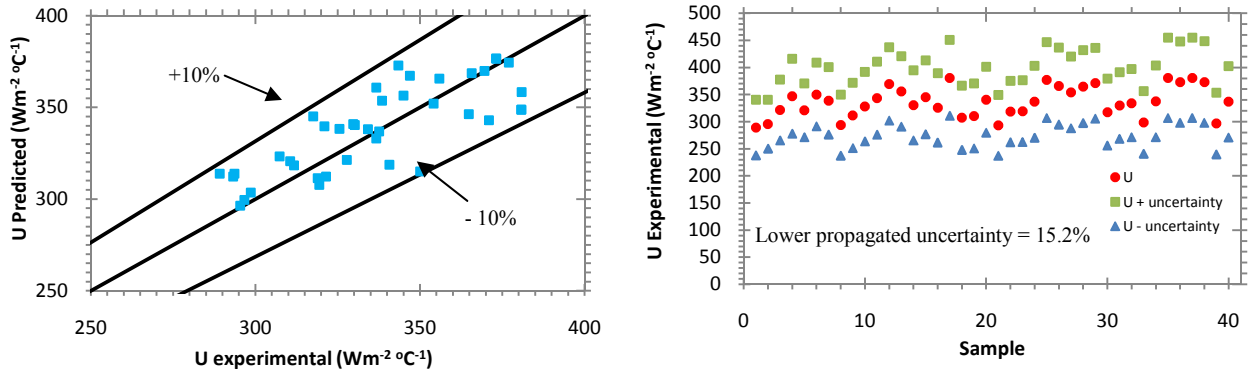

Figure 9. a) predicted versus experimental $\overline{U}$; b) propagated uncertainty for $\overline{U}$

The greater deviation found is lower than 10%. The greater deviation is lower measuring propagated uncertainty is 15.2%, like shows Fig 9b and it is greater than maximum deviation presented in Fig 9a for any of 40 samples.

4 CONCLUDING REMARKS

This work presented an experimental study on a small scale evaporative condenser. From obtained data, was proposed a new correlation in order to calculate the overall heat transfer coefficient based on geometric and operational conditions, only. These results show very good agreement between predicted and experimental values for 40 measuring samples. Two other real size evaporative condensers operating with R-717 were tested and the deviation found was lower than 13%. Just one correction is necessary to compensate the differences between thermophysical properties of the refrigerant fluids. It will be present in a future work that is being done.

5 ACKNOWLEDGEMENTS

The first author thanks to the financial support of CNPq (scholarship number 142589/2007-1)

6 REFERENCES

Acunha Jr., I. C. Walther, F. M., Smith Schneider, P., Beyer, P., 2010, Experimental analysis of an evaporative condenser, 13th Brazilian Congress of Thermal Sciences and Engineering, Uberlândia, Brazil.

ANSI/ASHRAE 64-1995, 1995, Methods of Testing Remote Mechanical-Draft Evaporative Refrigerant Condensers. Atlanta.

ASHRAE Handbook Fundamentals - American Society of Heating, Refrigerating and Air-Conditioning Engineers, 2005, Atlanta, GA.

ASHRAE Handbook HVAC Systems and Equipment - American Society of Heating, Refrigerating and Air-Conditioning Engineers, 2000, Atlanta, GA.

Bejan, A., 1995, Convection Heat Transfer, John Wiley & Sons, 2nd ed., New York.

Chato, J.C., 1962, Laminar condensation inside horizontal and inclined tubes, ASHRAE Journal, No.4, pp. 52-60.

Dreyer A. A., Erens, J. P., 1990, Heat and mass transfer coefficient and pressure drop correlations for a crossflow evaporative cooler, Proceedings, International Heat Transfer Conference, Vol 6, pp 233-238, Jerusalem.

El Hajal, J., Thome, J. R., Cavallini, 2003, A., Condensation in horizontal tubes, part 1: two flow pattern map, International Journal of Heat and Mass Transfer, Vol. 46 pp. 3349–3363.

Engineering Equation Solver <www.fchart.com>

Facão, J. M. R. V., 1999, Comportamento Térmico de Torres de Arrefecimento Indirectas para Aplicação a Sistemas de Arrefecimento Ambiente, Dissertação de Mestrado, Universidade do Porto.

Kattan, N., Thome, J.R., Favrat, D., 1998, Flow boiling in horizontal tubes: Part 1—Development of a diabatic two phase flow pattern map, J. Heat Transfer, Vol.120, pp.140–147.

Leidenfrost, W., Korenic, B. Evporative Cooling and Heat Transfer Augmentation Related to Reduce Condenser Temperatures, Heat Transfer Engineering, v. 3, p. 38-59, 1982.

Mizushina, T., Ito, R., Miyashita, H., Experimental study of an evaporative cooler, International Chemical Engineering, v. 4, p. 727-732, 1967.

Niitsu, Y., Naito, K., Anzai, T., 1967, Studies on Characteristics and design procedure of evaporative coolers, Journal of SHASE, Vol. 41 (12).

Parker, R. O., Treybal, R. E., 1961, The Heat, Mass transfer characteristics of evaporative coolers, Chemical Engineering Progress Symposium Series, v. 57,p.138-149.

Rouhani Z., Axelsson E., 1970, Calculation of void volume fraction in the subcooled and quality boiling regions, Int. J. Heat Mass Transfer Vol. 13, pp. 383–393.

Thome, J. R., Hajal, J. El, Cavallini, A., Condensation in horizontal tubes, part 2: new heat transfer model based on flow regimes, International Journal of Heat and Mass Transfer, v. 46, p. 3365–3387, 2003.

Zalewski, W., Gryglaszewski, P. A., Mathematical model of heat and mass transfer process in evaporative fluid coolers, Chemical Engineering and Processing, v. 36, p. 271-280, 1997

7 RESPONSIBILITY NOTICE

The authors are the only responsible for the printed material included in this paper.